Earth and Planetary Science Letters 464 (2017) 35–45

Contents lists available at ScienceDirect

Earth and Planetary Science Letters

www.elsevier.com/locate/epsl

Seismicity rate increases associated with slow slip episodes prior to the 2012 M_w 7.4 Ometepec earthquake

Harmony V. Colella [a,b,1], Stefany M. Sit [a,2], Michael R. Brudzinski [a,*], Shannon E. Graham [c,3], Charles DeMets [c], Stephen G. Holtkamp [a,4], Robert J. Skoumal [a], Noorulann Ghouse [a,5], Enrique Cabral-Cano [c], Vladimir Kostoglodov [d], Alejandra Arciniega-Ceballos [d]

[a] Department of Geology and Environmental Earth Sciences, Miami University, United States
[b] School of Earth and Space Exploration, Arizona State University, United States
[c] Department of Geoscience, University of Wisconsin–Madison, United States
[d] Instituto de Geofísica, Universidad Nacional Autónoma de México, Mexico

ARTICLE INFO

Article history:
Received 9 June 2016
Received in revised form 20 December 2016
Accepted 22 December 2016
Available online 23 February 2017
Editor: P. Shearer

Keywords:
earthquakes
tremor
slow slip
Mexico
subduction
swarm

ABSTRACT

The March 20, 2012 M_w 7.4 Ometepec earthquake in the Oaxaca region of Southern Mexico provides a unique opportunity to examine whether subtle changes in seismicity, tectonic tremor, or slow slip can be observed prior to a large earthquake that may illuminate changes in stress or background slip rate. Continuous Global Positioning System (cGPS) data reveal a 5-month-long slow slip event (SSE) between ~20 and 35 km depth that migrated toward and reached the vicinity of the mainshock a few weeks prior to the earthquake. Seismicity in Oaxaca is examined using single station tectonic tremor detection and multi-station waveform template matching of earthquake families. An increase in seismic activity, detected with template matching using aftershock waveforms, is only observed in the weeks prior to the mainshock in the region between the SSE and mainshock. In contrast, a SSE ~15 months earlier occurred at ~25–40 km depth and was primarily associated with an increase in tectonic tremor. Together, these observations indicate that in the Oaxaca region of Mexico shallower slow slip promotes elevated seismicity rates, and deeper slow slip promotes tectonic tremor. Results from this study add to a growing number of published accounts that indicate slow slip may be a common pre-earthquake signature.

1. Introduction

The megathrust fault in subduction zones, which is host to the world's largest earthquakes, exhibits several types of seismic and slip behavior. Earthquakes, or stick-slip behavior, typically occur at shallow depth (<~25 km), while aseismic continuous creep, or stable sliding, typically occurs deeper along the plate interface (>~25 km). Recent studies have revealed episodic tremor and slip (ETS) can form a transition zone between stick-slip and stable sliding along the plate interface at depths of ~25 km to as much as 80 km depth (Rogers and Dragert, 2003; Schwartz and Rokosky, 2007). Geodetic evidence of transient deformation reveals slow slip events (SSEs) are often accompanied by a tremor signal, commonly referred to as tectonic tremor. Matched-filter template scanning reveals tectonic tremor is an outcome of intense swarms of low-frequency earthquakes (e.g., Shelly et al., 2007) more easily triggered than traditional seismicity (Rubinstein et al., 2007; Thomas et al., 2009). Other studies show swarms of traditional earthquakes occur during SSEs (Crescentini et al., 1999; Delahaye et al., 2009; Linde et al., 1996; Lohman and McGuire, 2007; Montgomery-Brown et al., 2009; Ozawa et al., 2007; Vidale et al., 2011; Vallée et al., 2013). Both observations are consistent with models that suggest SSEs along a megathrust transfer stress to adjacent stick-slip sections of the plate interface, which increases the probability of seismicity, whether it be increased seismicity rates or a large-to-great earthquake (Dragert et al., 2004; Mazzotti and Adams, 2004; Colella et al., 2011; Segall and Bradley, 2012). Modeling efforts also complement laboratory experiments (Scholz et al., 1972) and numerical simulations (Tse and Rice, 1986; Kato and Hirasawa, 1999) that suggest large earthquakes can be preceded by small amounts of stable slip. A central focus since

* Corresponding author.
E-mail address: brudzimr@miamioh.edu (M.R. Brudzinski).
[1] Now at University of California, Berkeley.
[2] Now at University of Illinois Chicago.
[3] Now at Harvard University.
[4] Now at University of Alaska – Fairbanks.
[5] Now at Oklahoma Geological Survey.

http://dx.doi.org/10.1016/j.epsl.2016.12.032
0012-821X/

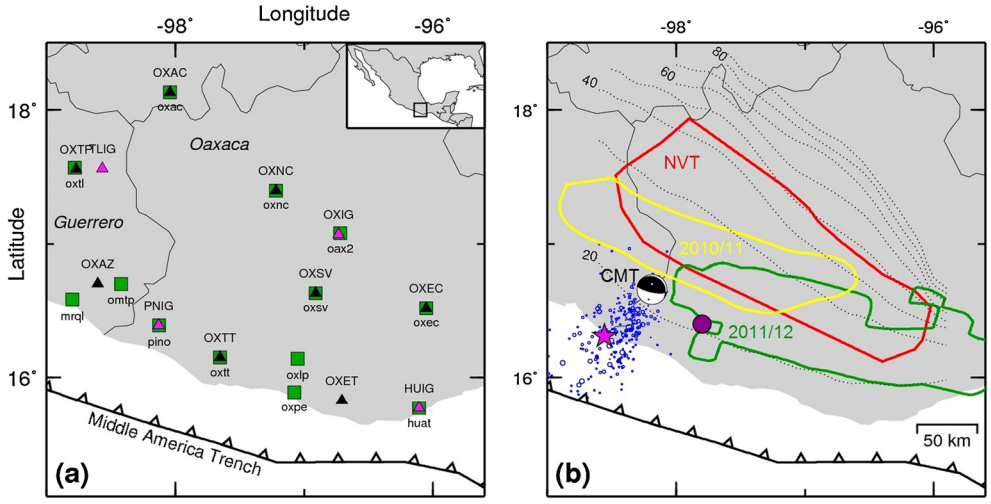

Fig. 1. A map of the study area: Oaxaca region, southern Mexico. State borders are plotted as solid lines. (a) The location of cGPS (green squares, lowercase names) and seismic stations (black triangles represent temporary stations and pink triangles represent permanent stations, upper case names). (b) The various forms of seismic and slip behavior, and the slab depth contours (dotted lines) (Fasola et al., 2016). The 2010–2011 SSE (yellow curve, Graham et al., 2015) was correlated with tectonic tremor (red curve, Fasola et al., 2016; see also Fig. S3). The 2011–2012 SSE (green curve; Graham et al., 2014), which was active immediately prior to the M_w 7.4 Ometepec earthquake. The USGS epicenter and CMT focal mechanism are plotted at the original USGS epicenter. The epicenter determined by the local network is updip of the USGS location (pink star); repeating earthquakes (blue circles, Fasola et al., 2016) detected with the template matching method on Ometepec aftershocks; and a seismic swarm first detected in 2006 near the downdip edge of the seismogenic zone (purple circle, Skoumal et al., 2016). (For interpretation of the references to color in this figure legend, the reader is referred to the web version of this article.)

the discovery of SSEs has been to detect and identify connections between SSEs and large megathrust earthquakes.

The March 20, 2012 M_w 7.4 Ometepec earthquake off the coast of southern Mexico occurred at a depth of ~15 km along the subduction megathrust with a pure thrust focal mechanism and aftershocks distributed along the subduction interface (Figs. 1 and S1, Supplementary Material) (UNAM Seismology Group, 2013). The Ometepec earthquake provides a unique opportunity to investigate the patterns of slow slip, tremor, and changes in seismicity rates prior to a large earthquake. This study describes the history of SSEs in the Oaxaca region of Mexico, which includes a SSE immediately preceding the Ometepec earthquake and examines the evidence for tremor or changes in seismicity rates prior to the earthquake. The study also investigates spatial and temporal patterns of seismicity in advance of the Ometepec earthquake. Finally, the observations are considered in the context of other studies that show potential relationships between slow slip, tremor, increased seismicity rates, and large earthquakes.

2. Previous geodetic and seismic observations

A network of continuous Global Positioning Stations (cGPS) and seismic stations have been operating in the Oaxaca region since 1993. 14 cGPS were installed between 1993 and 2011, and 7 three-component broadband seismometers were installed in 2006 (Fig. 1a). 2 additional stations were deployed in 2008 to the west of Oaxaca in eastern Guerrero, and 5 additional stations were permanently added in and around the Oaxaca state to from the Servicio Sismológico Nacional (SSN) array achieve a station spacing of ~70 km (Fig. 1a).

cGPS solutions indicate a northward long-term, interseismic strain accumulation and a southward strain release during SSEs (Brudzinski et al., 2007; Correa-Mora et al., 2009). Since 1993, SSEs in the Oaxaca region were documented to occur every 1–2 years with durations of ~2–4 months (Brudzinski et al., 2007). Geodetic inversions for the SSEs in 2004, 2005/6, 2007, 2008/9, and 2011/12 indicate that SSEs occurred in the transition zone downdip of the seismogenic zone defined by historic earthquakes (Fig. 1b) (Correa-Mora et al., 2009; Graham et al., 2014, 2015). Conversely, the 2010/11 SSE occurred further inland and downdip of the typical SSEs observed in Oaxaca (Fig. 1b; Graham et al., 2015).

The first study to exploit seismic data from this network identified tectonic tremor episodes throughout 2006–2007 that lasted a few days, occurred as often as every 2–3 months (Brudzinski et al., 2010). Tremor locations defined a trench-parallel band immediately downdip of SSE locations previously determined by cGPS inversions (Fig. 1b and Fig. S3). The observed tectonic tremor did not correlate temporally with observed SSEs. This observation resembles those from Nankai in Japan where only weak amounts of tectonic tremor are observed during large, long SSEs at ~20–30 km depth detected with cGPS and an abundance of tectonic tremor is observed during small, short SSEs at ~30–40 km depth detected with tiltmeters (Obara et al., 2004; Hirose and Obara, 2005). Since such high precision geodetic instruments are not available in Oaxaca, the typical short duration tectonic tremor may be coincident with the small, short, deep slow slip that occurs below the current resolution of the cGPS (Brudzinski et al., 2010).

More recently, Fasola et al. (2016) analyzed seismic data from the local network from 2006 to 2012, which includes the Ometepec earthquake and its aftershock sequence, to construct a catalog of earthquakes for the region and update tremor locations to determine the geometry of the plate interface. The distribution of well-located earthquakes delineated the geometry of the subducting plate and revealed a sharp bend in a shallow to steeply dipping slab from western to eastern Oaxaca (Fig. 1b, dotted lines). The updated catalog of tremor distributions (Fasola et al., 2016) together with cGPS measurements (Graham et al., 2015) showed SSEs propagate across the sharp bend in the subducting plate, which indicated the plate is not torn in this location.

3. Observations prior to the Ometepec earthquake

The March 20, 2012 M_w 7.4 Ometepec earthquake occurred off the coast of the Oaxaca region of Mexico along the subduction megathrust. The USGS location of the event was at the downdip edge of the seismogenic zone (Fig. 1b), close to the western limit of the preceding SSE (described below). However, the first motions from the local seismic network indicate the earthquake initiated ~30 km updip (Fig. S1, Supplementary Material), significantly shal-

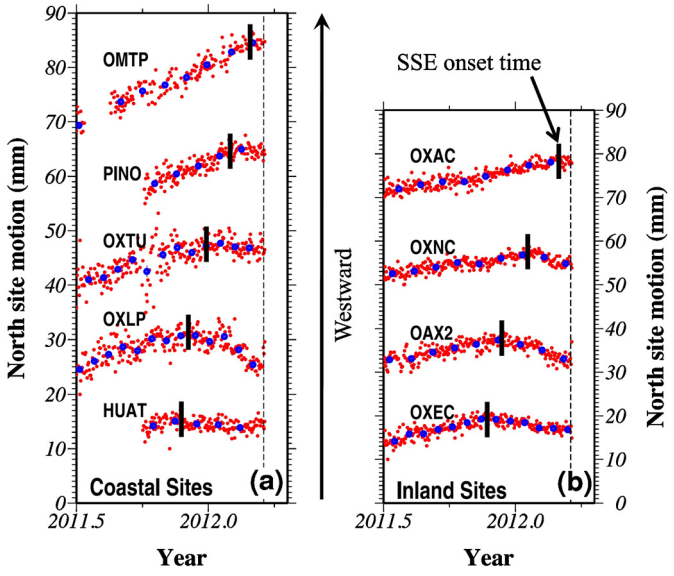

Fig. 2. North component of motion for selected (a) coastal and (b) inland cGPS stations during the 2011/12 SSE (after Graham et al., 2014). Dashed line denotes time of the mainshock. Vertical black bars indicate approximate SSE onset time. From east to west (bottom to top of panels), the SSE onset times become progressively later and begin only several weeks before the Ometepec earthquake at the two westernmost sites OMTP and OXAC.

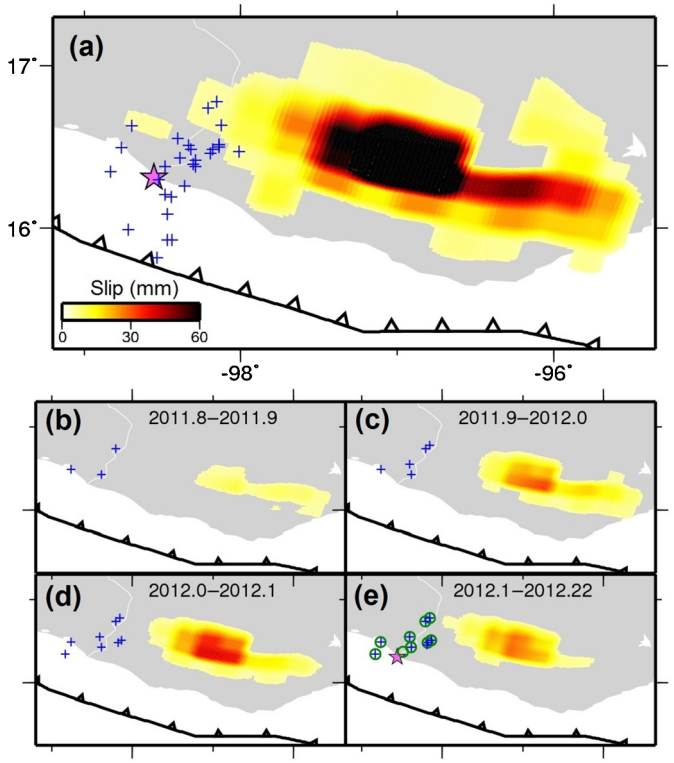

Fig. 3. (a) Best-fit slow slip solution from cGPS modeling (Graham et al., 2014), which illustrates the cumulative slow slip from November 1, 2011 to March 12, 2012 Ometepec earthquake (pink star). The blue crosses represent the location of aftershocks used as templates to construct earthquake families. (b–e) Monthly time steps of slow slip and template matching results that illustrate activity of aftershock families before the mainshock. Only families that experience more than 15 events during the time frame are shown. Green circles in the final time frame show nearly all families were active the week before the Ometepec earthquake. (For interpretation of the references to color in this figure legend, the reader is referred to the web version of this article.)

lower than the updip limit of the SSE (Figs. 1b and 3a). A data gap occurred on several seismic stations from late 2009 to early 2010, so this study focuses on data from June 2010 through the aftershock sequence for the Ometepec earthquake.

3.1. Geodetic observations

The 2011/12 SSE was investigated in detail by Graham et al. (2014) since it occurred near the source region of the Ometepec earthquake in the months leading up to the mainshock. We recount the key results as it motivates the seismological analysis in the current study. Slow slip was first detected in early November 2011 at the two easternmost coastal and inland sites, HUAT and OXEC, respectively (Fig. 2). Slip was then detected on stations progressively farther northwest at increasingly later times. Slip only began at site OMTP, the station nearest the epicenter, weeks before the earthquake and was ongoing at the time of the earthquake.

Fig. 3 shows best-fit space-time evolution of slip for the 2011/12 SSE determined by Graham et al. (2014). The results indicated a westward migration of slip for ~300 km along-strike (Fig. 3). The SSE started in the eastern and central regions of Oaxaca in November 2011, migrated westward below central Oaxaca in December and January 2012, which was also when the majority of the slip occurred, and moved to the far western regions of Oaxaca in February and March 2012, downdip from the imminent Ometepec earthquake (Fig. 3). Slip primarily occurred between depths of 20 and 40 km and closely followed the 20 km updip boundary of the transition zone. The cumulative surface displacement from cGPS range from a few mm to 10 mm (Fig. 2), where the largest displacements occurred near the midpoint of the network. The cumulative equivalent moment magnitude was M_w 6.9, with a maximum slip of ~100 mm approximately 125 km east of the earthquake epicenter (Fig. 3a).

3.2. Seismic observations

Previous studies of SSEs and seismicity have suggested possible spatial and temporal changes in tectonic tremor and earthquakes may occur prior to large-to-great earthquakes (see Section 4 for details). This section discusses a variety of seismic observations (e.g., tectonic tremor, repeating earthquakes, changes in earthquake rates) prior to the Ometepec earthquake and coincident with the 2011–2012 SSE. Based on the spatial offset between the SSE and the hypocenter determined from the local network, seismicity that may have assisted the transfer of stress updip and potentially triggered the Ometepec earthquake is of specific interest.

3.2.1. Tectonic tremor

To detect tectonic tremor, a single station, we applied a frequency scanning detection algorithm developed for Cascadia to seismic data from the local network in the Oaxaca region to exploit the unique frequency content of tectonic tremor (2–5 Hz) and reduce possible false detections from cultural noise and local seismicity (Sit et al., 2012). We filtered data with three frequency ranges to identify the seismic activity observed: tectonic tremor (2–5 Hz), local seismicity (10–15 Hz), and cultural noise (0.01–0.2 Hz). While tremor is typically present throughout 1–8 Hz, a narrower range of 2–5 Hz avoids influences from other signals. The algorithm calculates a ratio of amplitudes at different frequencies to amplify the low frequency signature of tectonic tremor, while also down weighting local seismicity and cultural noise. We determined an overall ratio value for each nighttime hour and then established a detection threshold of 2-sigma over the mean for a given year (Fig. 4a). To estimate tremor activity for a given day, the number of hours detected from nighttime analysis were doubled. For a network-wide tremor detection (Fig. 5a), two or more nearby single stations were required to have a positive detection during the same hour.

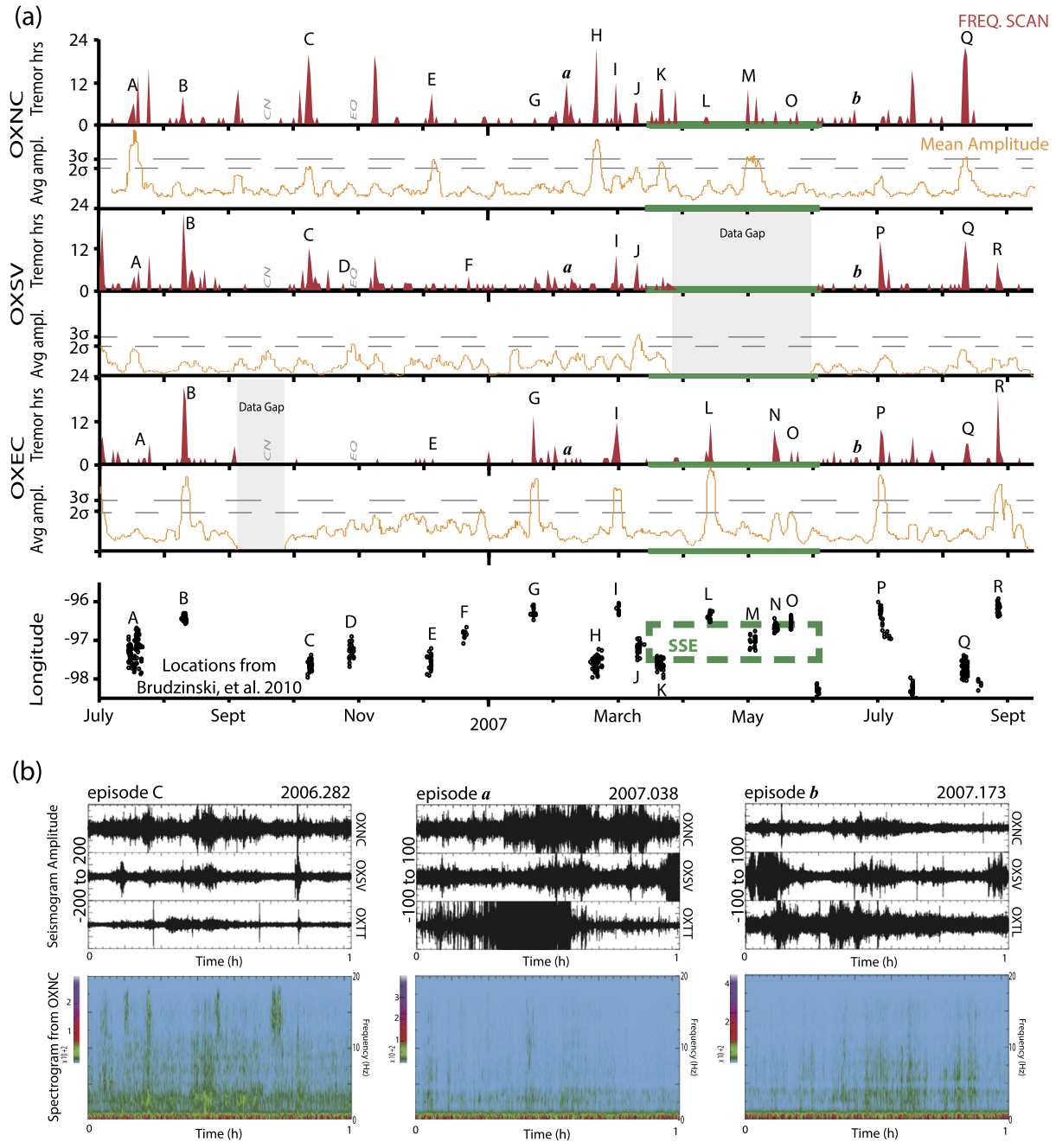

Fig. 4. (a) Comparison of results from single station frequency scanning and mean amplitude processing at OXNC, OXSV, and OXEC. Upper-case alphabetical letters indicate tremor episodes that have been located using a semi-automatic method in the bottom row (Brudzinski et al., 2010). Lower-case letters indicate examples of newly detected tremor episodes that have been visually verified. Grayed out letters indicate cultural noise and local earthquakes (verified in Fig. S1) that have been successfully avoided. (b) Tremor detections are verified through coherent activity observed from 2 to 5 Hz filtered seismograms from nearby stations along with spectrogram analysis from station OXNC for 1-hour sample of data.

Single station frequency scanning results produced comparable detections to single station mean amplitude scanning algorithms from Brudzinski et al. (2010) in this region. Fig. 4 shows results for frequency scanning from mid-2006 to mid-2007, which were compared to mean amplitude processing for stations OXNC, OXSV, and OXEC. Results from a semi-automated tremor location technique were also available during times of prominent tremor energy (located events are labeled with upper-case alphabetical letters). Single station frequency scanning produced similar if not more clearly distinguished tremor events than the mean amplitude processing detection method. Most noticeably at station OXSV, where mean amplitude processing has difficulty detecting any events over 2-sigma, the frequency scanning method detected distinct events lasting multiple hours. Frequency scanning also revealed several new short duration tremor episodes. Fig. 4b shows examples of two newly identified episodes, which were verified by inspection of nearby station seismograms for correlated activity and examination of spectrograms for sustained amplitudes in the tremor frequency range. This case resembles that of more prominent tremor episode C. The Supplementary Material provides evidence that this technique avoids detection of cultural noise and local earthquakes similar to Sit et al. (2012) (Fig. S2).

Prior analysis of the first 14 months of the local deployment by Brudzinski et al. (2010) found tectonic tremor occurs for a short duration (2–10 days) as often as 2–3 months, but poorly correlates with cGPS-detected SSEs. While we identified

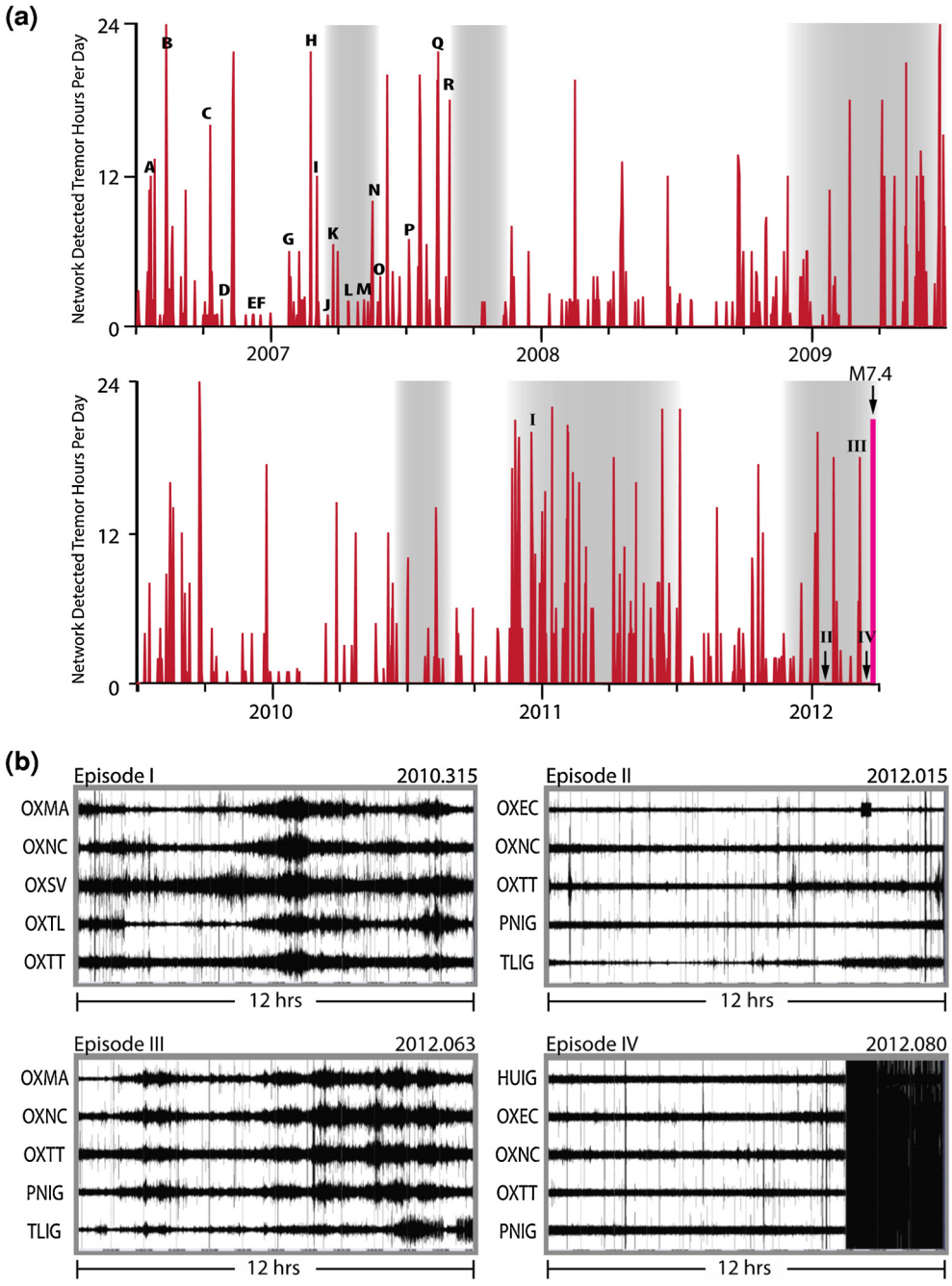

Fig. 5. (a) Network-wide tremor detections spanning mid-2006 until the Ometepec mainshock. Number of hours per day with positive tremor detections based on the technique of Sit et al. (2012) that uses ratios of amplitudes at different frequencies to determine whether tremor occurs in any given hour. The arrow marks the time of the M_w 7.4 Ometepec earthquake. Gray bars represent the approximate duration of geodetically observed SSEs from Graham et al. (2014, 2015). Alphabetically labeled events are located tremor events from Fig. 2 and roman numerals represent dates that are verified through filtered seismograms at multiple stations. (b) 12-h filtered seismograms for the labeled dates. Positive detections, episodes I and III, show correlated emergent activity at multiple stations. Null detections, episodes II and IV, experience less activity, but show evidence for several short duration, instantaneous local earthquakes that appear as very thin vertical lines. The y-axis for station seismograms range from −100 to 100 nm through −1500 to 1500 nm to best reflect correlated signals across multiple stations.

some tectonic tremor during the 2011/12 SSE, it is near the background rate (Fig. 5). Visual inspection of bandpass-filtered seismograms confirms the sparse tremor activity during the SSE and in the months prior to the Ometepec earthquake, which includes the several hours immediately prior to the earthquake (Episode IV in Fig. 5). Episodes II and III during the SSE are examples of a null and positive detection, respectively, which have distinctly different patterns (Fig. 5). These examples also illustrate the short duration, large amplitude activity of local earthquakes (II), and the long duration, emergent activity of tremor (III).

Tectonic tremor is detected on less than 15% of the total days during 5 of the 6 most recent SSEs in the Oaxaca region (Fig. 5). The one exception is the 2010/11 SSE, the last completed SSE prior to the Ometepec earthquake. Frequency scanning detected tremor on 60% of the days with an average tremor rate of 7 h per day. We found several days with up to 20 h of tremor, and a peak of 100 h of tremor in a week (Figs. 5a and 6a). While the tremor rate does not appear to increase during the 2011/12 SSE, the updip location of the SSE led us to investigate of the possibility of increased seismicity prior to the M_w 7.4 Ometepec earthquake.

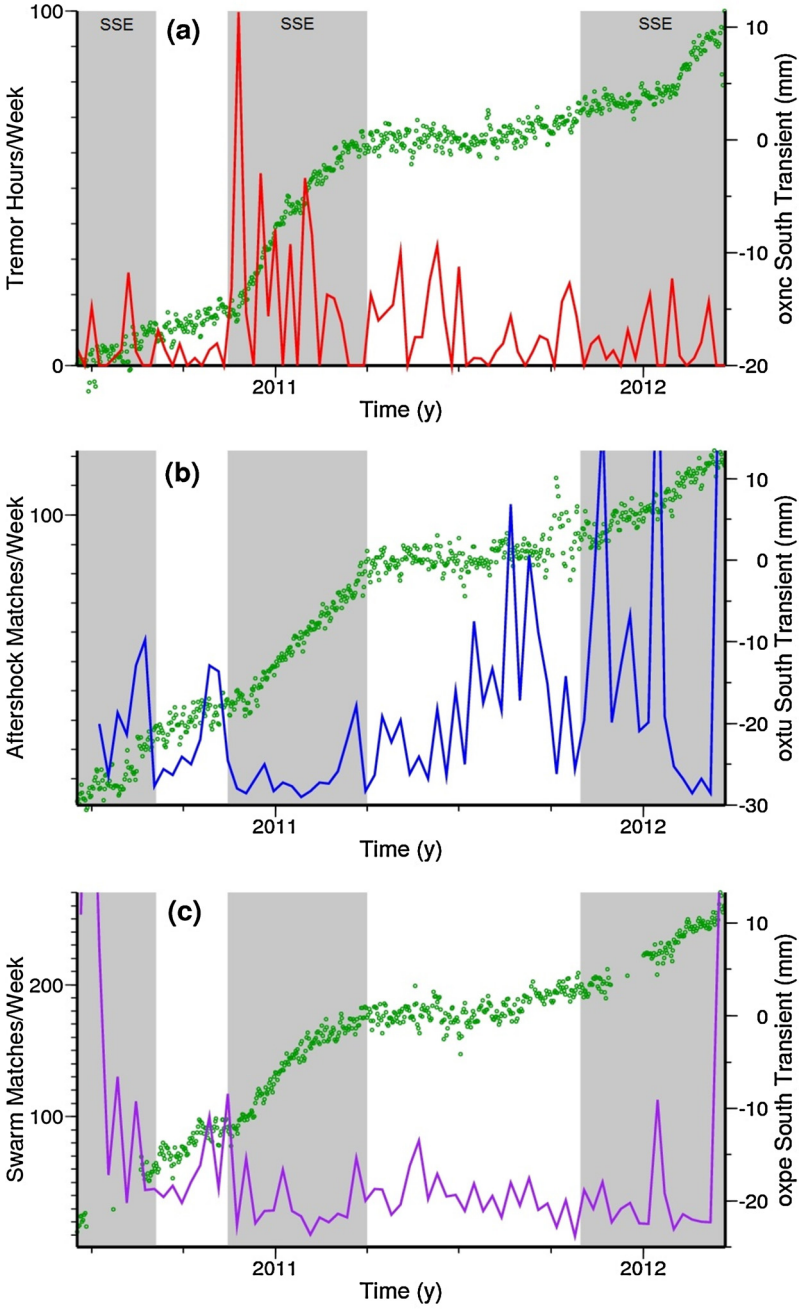

Fig. 6. Comparison of geodetic and seismic signatures in the Oaxaca region in the 2 years leading up to the Ometepec earthquake. This time frame was chosen for analysis as there are no data gaps for the seismic analysis. Green dots show transient motions associated with slow slip calculated by correcting cGPS north displacements to remove the long-term northward trend associated with megathrust strain accumulation. Colored lines show weekly rates of detected seismicity or tremor. (a) Comparison with number of hours of detected tectonic tremor per week (red) using a ratio of amplitudes from different frequency bands. (b) Comparison with number of matched earthquakes per week using the Ometepec aftershocks as template events (blue). (c) Comparison with number of matched earthquakes per week using the 2006 downdip earthquake swarm as template events (purple). (For interpretation of the references to color in this figure legend, the reader is referred to the web version of this article.)

3.2.2. Earthquake families

The Ometepec aftershock sequence provides a robust catalog of earthquakes, which we utilized to help illuminate the time history of seismicity in and around the Ometepec rupture zone. A lack in prominent tremor activity and the occurrence of a shallow SSE prior to Ometepec event motivated our investigation of seismicity rates, similar to Delahaye et al. (2009) where earthquake swarms are observed to be associated with shallower SSEs. We employed a multi-station waveform matching technique to identify times when events with similar waveforms, or earthquake families, are active prior to the Ometepec mainshock (e.g., Shelly, 2009; Skoumal et al., 2015). The technique allows for a lower magnitude detection threshold for seismicity in our region of interest. Since it was computationally infeasible to process the entire Oaxaca earthquake catalog over multiple years, we investigated three catalog of earthquake families: all cataloged aftershocks within first 24 hours of the Ometepec mainshock that were primarily constrained to the mainshock rupture area, aftershocks with clear waveforms in the first 1–10 days of the mainshock that covered a broader area, and earthquakes in the 2006 swarm region to the east (Fig. 1).

Fasola et al. (2016) manually reanalyzed P- and S-wave arrivals for each cataloged earthquakes and inverted for a source location with a locally appropriate velocity model. We constructed templates using various station combinations to optimize the matching

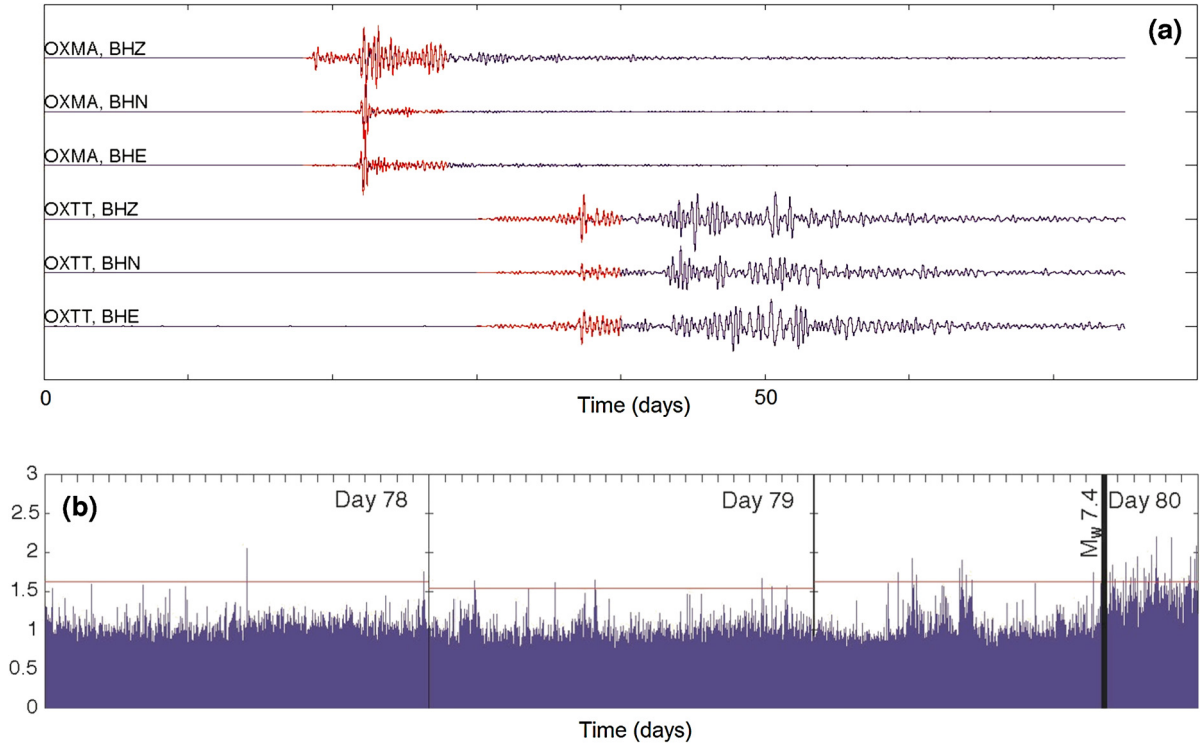

Fig. 7. (a) Example waveforms of template 13 from stations OXMA and OXTT and for all 3 components. The red outlines the portion of waveform around the S-wave selected for cross correlation. (b) Detector time series, where results are combined from stations OXMA and OXTT, for 3 days prior to the Ometepec earthquake displays summed correlation coefficient values. While the maximum cross correlation coefficient for a 2-station detector is 6, none of the values for this region are very large; therefore the y-axis is limited to 0 to 3. The red line is the detection threshold for each day. (For interpretation of the references to color in this figure legend, the reader is referred to the web version of this article.)

performance (e.g., Skoumal et al., 2015), and found the best results using stations OXMA and OXTT. Other potential stations in the local network have data gaps or higher noise levels over the time frame investigated in this study that degraded the template matching performance. All three station components for these stations have a unique waveform that preserves the time offset between arrivals at different stations (Fig. 7). Each template waveform was downsampled to 40 samples/s, bandpass filtered between 5 and 15 Hz, and cross-correlated against its respective station-component data stream from June 2010 until the mainshock. The correlated results are summed based on the time offsets and divided by the number of data streams to form the network normalized correlation coefficient (NNCC). Similar to previous template matching studies (e.g., Skoumal et al., 2015), the detection threshold was set at 15 times the median absolute deviation (MAD) of the daily NNCC to minimize both false negatives and false positives. Theoretically, correlation of a randomly generated template against a random year-long signal at 40 samples/s would result in ~1 false positive based on what 15 × MAD represents. We determined local magnitudes through a Richter scale approach:

$$M_L = \log 10[\mathbf{A}/\mathbf{A_0}]$$

For each station and component in our template, we calculated the median scale factor ($\mathbf{A_0}$) using the filtered S waveform amplitudes ($\mathbf{A}$) and catalog magnitudes for all events from Fasola et al. (2016). For each matched event, we calculated a magnitude from the scale factor and S waveform amplitude at each station and component, and took the median value as our final magnitude.

Fig. 8 shows waveforms for matches from one template event, which illustrates the earthquakes in a family are similar but typically not identical. This suggests the detected seismicity in Oaxaca represents groups of events with similar but not identical source locations.

First, we focused on using aftershocks during the first 24 hours following the mainshock as templates to look for any patterns of earthquake families through time and potential relationships to SSEs (Fig. 5b). We started with this set of templates because they were most likely represent slip within (or closest to) the mainshock rupture zone. Fig. 9a shows the magnitudes over time for template matched events. The frequency–magnitude distribution of matched events (Fig. 9b) is similar to that of individual template events (Fig. 9c) above the magnitude of completeness (M_c) of 3.0. The maximum likelihood estimate of the b-value of ~0.8 is similar in both cases with the same M_c, but there is a shallower slope for smaller magnitude matched events, which suggests that the template matching is not capturing smaller magnitude events ($<M_c$).

Fig. 9a shows a somewhat constant level of seismicity, with >10 matched events in all months analyzed, but there were several bursts of activity that suggest significantly higher seismicity rates. Fig. 6b illustrates the rate of seismicity per week we calculated from 2010 to immediately prior to the Ometepec earthquake based on earthquake families from the first 24 hours of aftershocks. The highest seismicity rates occurred during the 2011/12 SSE, which did not correlate with tectonic tremor (Fig. 6a). Conversely, lower weekly seismicity rates occurred during the 2010/2011 SSE (Fig. 6b), but this event did correlate well with tectonic tremor (Fig. 6a).

Templates from the first 10 days of aftershocks from the Ometepec earthquake cover a broad region up and downdip of the mainshock epicenter (Fig. 3a). Of the 36 templates identified, 27 showed an increase in activity during the 2011/12 SSE. Fig. 3b–e illustrates the most active templates (>15 matches in each time frame) during the months preceding the mainshock. It is important to note that throughout the SSE the active earthquake families were only located between the earthquake epicenter and the slow slip region; none of the earthquake families located updip of the

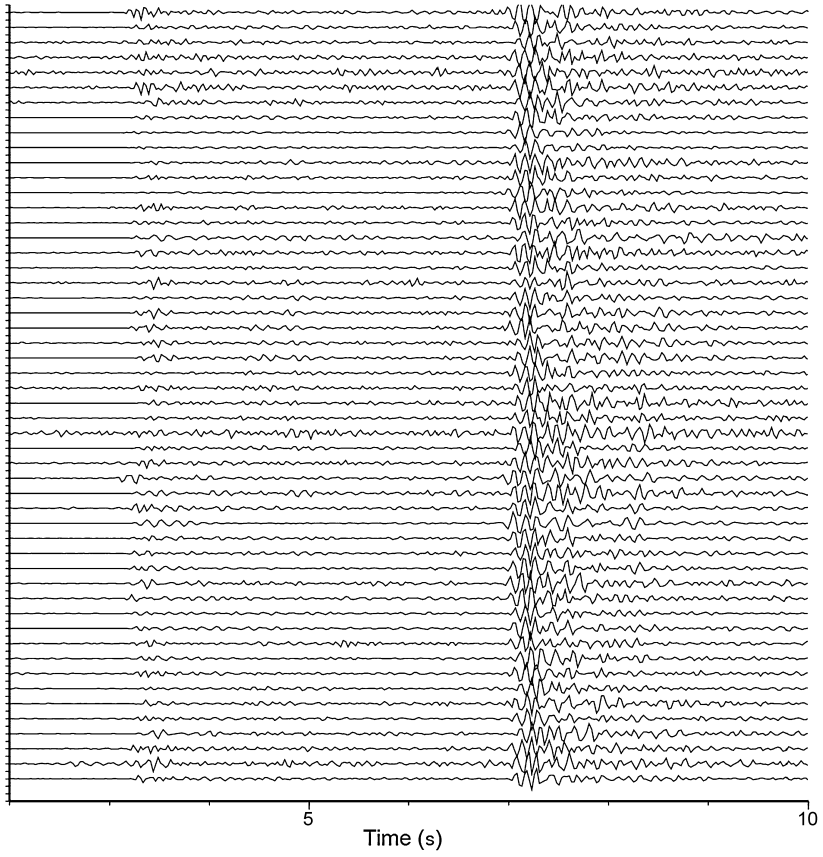

Fig. 8. Filtered, normalized OXMA-BHZ waveforms for the best matching events (MAD > 20) using a single aftershock of the Ometepec sequence as the template.

mainshock experienced any change in rates (Fig. 3b–e). At the beginning of the SSE when slip is furthest away from the mainshock, only 3 template families were active (Fig. 3b). As the amount of slip increases and migrated westward in December 2011 (Fig. 3c) and January of 2012 (Fig. 3d), more earthquake families became active and spatially filled the area between the SSE and earthquake epicenter. Interestingly, the number of active templates remained high even though the modeled amount of slip decreased in February and March (Fig. 3e). The green circles in Fig. 3e illustrate 14 templates were active the week prior to the earthquake, which includes the earthquake families closest to the epicenter of the mainshock that were not previously active during the SSE.

To help investigate if seismicity rate changes are associated with SSEs outside the Ometepec rupture zone, we also performed template matching on a documented earthquake swarm at the downdip edge of the seismogenic zone in 2006 about 50 km east of the mainshock (Fig. 1, purple circle) (Skoumal et al., 2016). Fig. 9d shows the magnitudes over time for earthquake families generated using the 2006 swarm events as templates. The frequency–magnitude distribution of matched events (Fig. 9e) is similar to that of template events alone (Fig. 9f) above a magnitude of completeness (M_c) of 2.0. The M_c for the 2006 swarm is lower than for the Ometepec aftershocks because of the proximity to station OXTT. Similar to results using the Ometepec aftershock templates, the maximum likelihood estimate of the b-value is also ~0.8 for both matches and templates using the same M_c, with a shallower slope for events below the M_c. Generally, the number of matched events per month was higher than that from the Ometepec aftershocks (Fig. 9a and d), but it is common for swarm regions to have higher seismicity rates. The rate of earthquake families from the swarm did not increase during the 2011–12 SSE, nor was there a noticeable increase in detected events during the 2010–11 SSE that correlated with tectonic tremor (Fig. 6c). However, an increased seismicity rate is observed during the SSE in mid-2010 at the beginning of reliable seismic recording analyzed in this study (Fig. 5c).

4. Evidence slow slip promotes seismicity

Analysis of seismic and cGPS data from the local network in the Oaxaca region of Mexico in our study has revealed changes in seismic behavior coincident with the 3 most recent SSEs. We detected an increase in the rate of earthquake families from the aftershock sequence of the Ometepec earthquake during the 2011–12 SSE (Fig. 6b). Both the earthquakes (~15–20 km depth) and the SSE (~20–35 km depth) occurred near the base of the seismogenic zone (Fig. 1b). Similarly, we detected an increase in the rate of earthquake families from a 2006 earthquake swarm during the mid-2010 SSE (Fig. 6c). The swarm earthquakes occurred at a slightly deeper depths (~20–25 km) (Fig. 1b), and the mid-2010 SSE occurred at depths between the shallow 2011–12 and deep 2010–11 SSEs (Graham et al., 2014, 2015). The rates of all earthquake families we investigated remained low during the 2010–11 SSE, which occurred deeper along the subduction zone interface (~23–40 km) (Fig. 1b). However there was an increase in tectonic tremor at depths of 25–60 km during the 2010/11 SSE. These observations resemble those from Nankai in Japan where only weak amounts of tectonic tremor were observed during long-term SSEs at ~20–30 km depth and an abundance of tectonic tremor was observed during short-term SSEs at ~30–40 km depth (Obara et al., 2004; Hirose and Obara, 2005). Additionally, the findings are similar to those for SSEs in New Zealand, where shallow SSEs were associated with earthquake swarms and not tectonic tremor (Delahaye et al., 2009). Cumulatively, these results indicate SSEs can promote slip on nearby patches of the subduction interface that results in either tremor or seismicity depending on the depth.

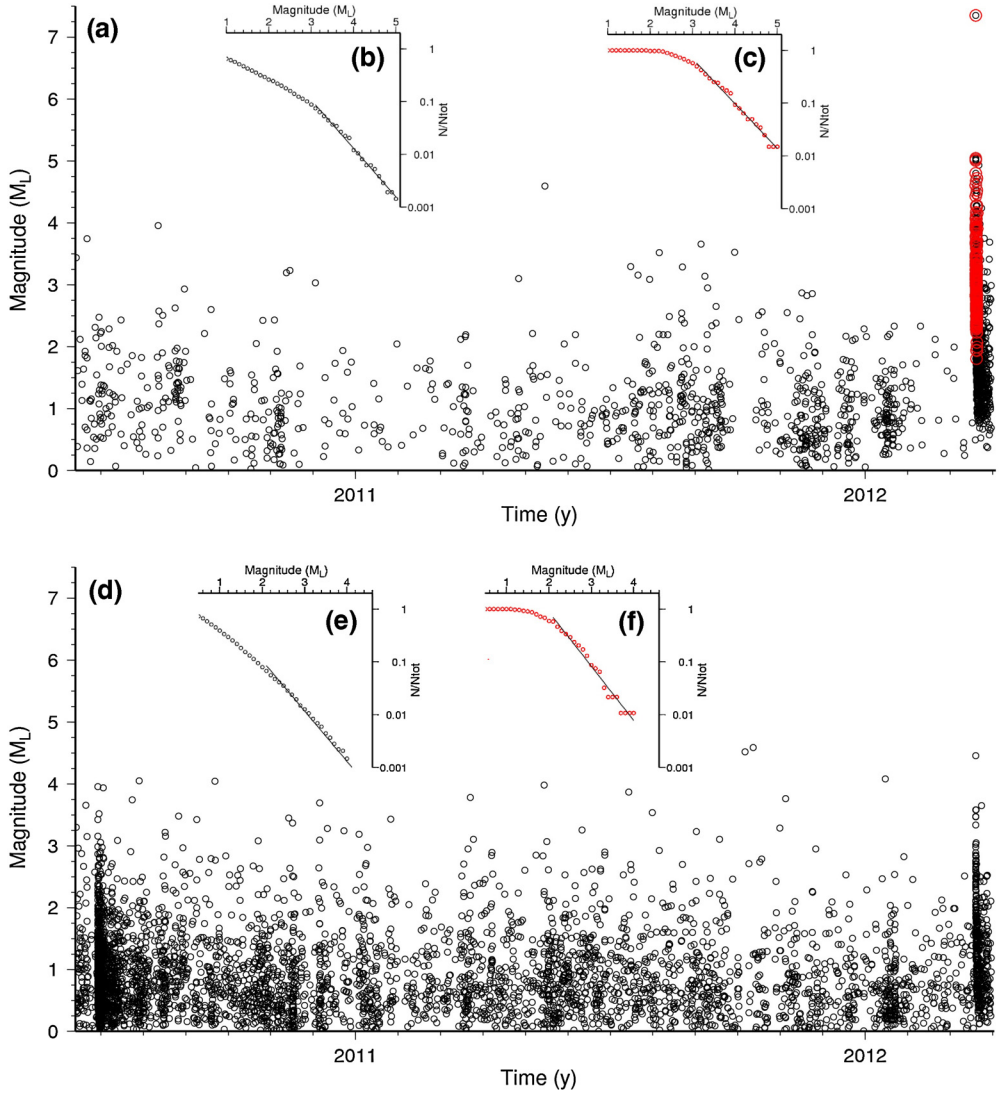

Fig. 9. Results of template matching from the first 24 hours of Ometepec aftershocks (a–c) and the 2006 swarm (d–f), showing templates (red) and matched events (black). (a) and (d) Local magnitudes over time, except for the mainshock. Template magnitudes are from the catalog of Fasola et al. (2016), match magnitudes are calculated relative to the template. (b) and (e) Frequency–magnitude distribution for matched events and templates. (c) and (f) Frequency–magnitude distribution for templates only. (For interpretation of the references to color in this figure legend, the reader is referred to the web version of this article.)

Results from this study add to the growing collection of SSEs that promote some form of seismic activity. At least 10 studies show geodetic or paleoseismic observations of slow slip (e.g., leveling, cGPS, strainmeter, tide gauge, pressure gauge, microfossils) before $M > 6$ earthquakes (Roeloffs, 2006; Ito et al., 2013) (Table S1, Supplementary Material). Additionally, at least 20 studies document swarms of smaller earthquakes coincident with geodetically-measured slow slip (Linde et al., 1996; Crescentini et al., 1999; Lohman and McGuire, 2007; Ozawa et al., 2007; Delahaye et al., 2009; Montgomery-Brown et al., 2009; Vidale et al., 2011; Vallée et al., 2013; Ruiz et al., 2014), and several more document tectonic tremor associated with slow slip (e.g., Ozawa et al., 2004; Shelly et al., 2007; Schwartz and Rokosky, 2007). If swarms of seismicity are taken as a proxy for slow slip, either in the form of earthquake swarms or tectonic tremor, there are an additional 6 reports of seismicity rate changes in advance of large earthquakes (Uchida et al., 2004; Shelly, 2009; Bouchon et al., 2011; Kato et al., 2012; Ruiz et al., 2014). Finally, there is also evidence that some aftershock sequences are driven by postseismic afterslip (e.g., Perfettini and Avouac, 2004; Hsu et al., 2006; Nadeau and Guilhem, 2009).

The temporal and spatial observations of slow slip and seismicity prior to the Ometepec earthquake provide an opportunity to investigate models for how slow slip can promote seismic activity. The two relationships most commonly attributed to triggered earthquakes are through dynamic stress or static stress transfer. Segall and Bradley (2012) proposed a model for dynamic stress transfer where slow slip partially propagates into the locked seismogenic zone and dynamically evolve into earthquake rupture. Because the Ometepec epicenter occurs ∼30 km updip from the geodetically detected SSE, an evolution from slow slip to earthquake rupture seems unlikely. This does not appear to be an uncommon observation as several other recent studies indicate SSEs increase seismicity despite spatial separation (Linde et al., 1996; Crescentini et al., 1999; Lohman and McGuire, 2007; Delahaye et al., 2009; Montgomery-Brown et al., 2009; Ozawa et al., 2007; Vidale et al., 2011; Vallée et al., 2013). Static stress models suggest SSEs transfer stress immediately updip of the slow slip region (Dragert et al., 2004) and that repeated SSEs cause a stress concentration at the base of the seismogenic zone (Colella et al., 2011), both of which may encourage earthquake initiation at the junction between slow slip and earthquake slip (Matsuzawa et al., 2010). The spatial offset of the Ometepec epicenter ∼30 km updip from

the SSE also suggests the amount of static stress change where the rupture initiates is quite small. Graham et al. (2014) calculate Coulomb stress changes from the 2011–12 SSE would be less than 0.01 bar at the epicenter if slow slip equal to or greater than 10 mm is used in the calculation. Larger positive stress changes (up to 0.03 bar) are predicted at the epicenter for solutions that are driven when slip greater than 5 mm is included in the calculation, but slip values this small may not be well resolved.

Nevertheless, increased rates of earthquake families between the epicenter and the SSE prior to the Ometepec earthquake occurred with no significant change in tremor activity at deeper depths. Similarly, a relatively shallow SSE in mid-2010 about 50 km east of the Ometepec earthquake promoted increased seismicity in the lower seismogenic zone but did not result in increased tremor activity. These observations suggest the effects of the SSE are concentrated in the region immediately updip from the SSE. While previous studies have suggested migrating small seismicity indicates the existence of a SSE that could be below the level of detectability (Kato et al., 2012; Kato and Nakagawa, 2014), an alternative hypothesis to stress triggering that may explain these observations is that a SSE liberates fluids as the slip breaks a hydrologic seal that forms in between episodes (Audet et al., 2009). As the freed fluid attempts to flow upward along the plate interface it would raise pore fluid pressures in the lower portion of the seismogenic zone and potentially lower the effective stresses enough to trigger seismicity. Evidence for or against this hypothesis should be the target of future studies.

Observations from the 2012 M_w 7.4 Ometepec earthquake are similar to those from several recent large-to-great earthquakes, including the 2011 M_w 9 Tohoku-Oki, 2012 M_w 7.6 Nicoya Peninsula, and 2014 M_w 8.1 Iquique earthquakes, where the mainshock was preceded by detectable slow slip, foreshock activity, and/or earthquake swarms (Ito et al., 2013; Kato et al., 2012; Ruiz et al., 2014; Kato and Nakagawa, 2014; Brodsky and Lay, 2014; Walter et al., 2015). These recent cases are noteworthy because they likely represent the best recorded large earthquakes due to the proliferation of seismic and geodetic monitors over the last decade. Moreover, the discovery of episodic tremor and slip a little over a decade ago has led to development of better techniques to discern the various signatures of slow slip. The improved observations and processing techniques may help explain why researchers are finding more evidence for relationships between slow slip and earthquakes than were previously observed.

Despite the growing body of evidence for pre-earthquake transients, geophysicists are naturally hesitant to rely on precursory phenomena as a predictive measure because none of the previously proposed phenomena have yet proven to be predictive at a statistical significant level (Hough, 2009). Slow slip phenomena are no exception, as many large earthquakes have no measured preseismic transient deformation (Roeloffs, 2006). While it is likely a SSE is not required for a large earthquake to nucleate, slow slip may be occurring below the detectability threshold of cGPS. For example, despite heavy instrumentation prior to the 2004 M_w 6 Parkfield earthquake, borehole strain data lacked evidence of a pre-earthquake slip transient (Langbein et al., 2006). However, a subsequent study revealed the presence of tectonic tremor and associated migration of seismicity in the 3 months prior to the earthquake, consistent with deep fault slip, which is undetectable in a strike-slip regime (Shelly, 2009). This scenario is similar to other recent observations that have identified subtle precursory signatures that have required advanced processing to uncover (e.g., Kato et al., 2012). Detailed investigations of increased seismicity, slow slip transients, and tectonic tremor are necessary to more thoroughly understand the relationship between these phenomena and large-to-great earthquakes.

The body of evidence collected thus far is sufficient to indicate that the occurrence of large earthquakes is possible during SSEs, and that it is imperative the geoscience community further investigate the relationship between SSEs and subsequent behavior prior to large-to-great earthquakes to create time-varying probabilistic hazard estimates. Such efforts require significant improvement of monitoring of transient slip and advanced real-time processing of seismicity to identify possible precursory activity and improve our ability to estimate potential increases in earthquake probabilities.

5. Conclusions

The three most recent SSEs in the Oaxaca region of southern Mexico are each associated with increased seismic activity relative to background rates. An elevated level of tremor is associated with the 2010–2011 deep SSE and increased rates of repeating earthquakes or earthquake families are associated with the mid-2010 and 2011–2012 shallow SSEs. This suggests deep SSEs that extend well below the downdip limit of the seismogenic zone are more commonly associated with tectonic tremor, while shallow SSEs are more commonly associated with increased rates of traditional earthquakes. The increase rate of repeating earthquakes associated with the 2011–2012 SSE, which was active at the time of the 2012 M_w 7.4 Ometepec earthquake, migrated updip from the SSE zone toward the epicentral region of the mainshock. These observations suggest the effects of the SSE are concentrated in the region immediately updip from the SSE. An alternative hypothesis to stress triggering that may explain these observations is that a SSE liberates fluids that flow upward along the plate interface, which may raise pore fluid pressures and lower the effective stress enough to trigger seismicity. In any case, results from this study add to the growing collection of SSEs that promote some form of seismic activity, such that additional studies are warranted to estimate the time-varying probabilistic hazards associated with SSEs.

Acknowledgements

This work was supported by NSF grants EAR-PF 114478 (HVC), EAR-0847688 (MB), and EAR-1114174 (CD), and an ASU-SESE Fellowship (HVC). We thank the many members of our institutions who have helped to collect the local seismic and cGPS data as well as the SSN for providing additional seismic data. Two anonymous reviewers provided constructive reviews and S. Fasola helped improve the quality of this manuscript.

Appendix A. Supplementary material

Supplementary material related to this article can be found online at http://dx.doi.org/10.1016/j.epsl.2016.12.032.

References

Audet, P., Bostock, M.G., Christensen, N.I., Peacock, S.M., 2009. Seismic evidence for overpressured subducted oceanic crust and megathrust fault sealing. Nature 457, 76–78. http://dx.doi.org/10.1038/nature07650.

Bouchon, M., Karabulut, H., Aktar, M., Ozalaybey, S., Schmittbuhl, J., Bouin, M.-P., 2011. Extended nucleation of the 1999 M_w 7.6 Izmit earthquake. Science 331, 877–880. http://dx.doi.org/10.1126/science.1197341.

Brodsky, E.E., Lay, T., 2014. Recognizing foreshocks from the 1 April 2014 Chile earthquake. Science 344, 700–702. http://dx.doi.org/10.1126/science.1255202.

Brudzinski, M., Cabral-Cano, E., Correa-Mora, F., DeMets, C., Márquez-Azúa, B., 2007. Slow slip transients along the Oaxaca subduction segment from 1993 to 2007. Geophys. J. Int. 171, 523–538.

Brudzinski, M.R., Hinojosa-Prieto, H.R., Schlanser, K.M., Cabral-Cano, E., Arciniega-Ceballos, A., Diaz-Molina, O., DeMets, C., 2010. Nonvolcanic tremor along the Oaxaca segment of the Middle America subduction zone. J. Geophys. Res. 115. http://dx.doi.org/10.1029/2008JB006061.

Colella, H.V., Dieterich, J.H., Richards-Dinger, K.B., 2011. Multi-event simulations of slow slip events for a Cascadia-like subduction zone. Geophys. Res. Lett. 38, L16312. http://dx.doi.org/10.1029/2011GL048817.

Correa-Mora, F., DeMets, C., Cabral-Cano, E., Diaz-Molina, O., Marquez-Azua, B., 2009. Transient deformation in southern Mexico in 2006 and 2007: evidence for distinct deep-slip patches beneath Guerrero and Oaxaca. Geochem. Geophys. Geosyst. 10. http://dx.doi.org/10.1029/2008GC002211.

Crescentini, L., Amoruso, A., Scarpa, R., 1999. Constraints on slow earthquake dynamics from a swarm in central Italy. Science 286, 2132–2134.

Delahaye, E.J., Townend, J., Reyners, M.E., Rogers, G., 2009. Microseismicity but no tremor accompanying slow slip in the Hikurangi subduction zone, New Zealand. Earth Planet. Sci. Lett. 277, 21–28. http://dx.doi.org/10.1016/j.epsl.2008.09.038.

Dragert, H., Wang, K., Rogers, G., 2004. Geodetic and seismic signatures of episodic tremor and slip in the northern Cascadia subduction zone. Earth Planets Space 56, 1143–1150.

Fasola, S., Brudzinski, M.R., Ghouse, N., Solada, K., Sit, S., Cabral-Cano, E., Arciniega-Ceballos, A., Kelly, N., Jensen, K., 2016. New perspective on the transition from flat to steeper subduction in Oaxaca, Mexico, based on seismicity, nonvolcanic tremor, and slow slip. J. Geophys. Res., Solid Earth 121. http://dx.doi.org/10.1002/2015JB012709.

Graham, S.E., DeMets, C., Cabral-Cano, E., Kostoglodov, V., Walpersdorf, A., Cotte, N., Brudzinski, M.R., McCaffrey, R., Salazar-Tlaczani, L., 2014. GPS constraints on the 2011–2012 Oaxaca slow slip event that preceded the 2012 March 20 Ometepec earthquake, southern Mexico. Geophys. J. Int. 197, 1593–1607. http://dx.doi.org/10.1093/gji/ggu019.

Graham, S., DeMets, C., Cabral-Cano, E., Kostoglodov, V., Rousset, B., Walpersdorf, A., Cotte, N., Lasserre, C., McCaffrey, R., Salazar-Tlaczani, L., 2015. Slow slip history for the Mexico subduction zone: 2005 through 2011. Pure Appl. Geophys., 1–21. http://dx.doi.org/10.1007/s00024-015-1211-x.

Hirose, H., Obara, K., 2005. Repeating short- and long-term slow slip events with deep tremor activity around the Bungo channel region, southwest Japan. Earth Planets Space 57, 961–972.

Hough, S., 2009. Predicting the Unpredictable: The Tumultuous Science of Earthquake Prediction. Princeton University Press.

Hsu, Y.J., Simons, M., Avouac, J.P., Galetzka, J., Sieh, K., Chlieh, M., Natawidjaja, D., Prawirodirdjo, L., Bock, Y., 2006. Frictional afterslip following the 2005 Nias-Simeulue earthquake, Sumatra. Science 312, 1921–1926.

Ito, Y., Hino, R., Kido, M., Fujimoto, H., Osada, Y., Inazu, D., Ohta, Y., Iinuma, T., Ohzono, M., Miura, S., Mishina, M., Suzuki, K., Tsuji, T., Ashi, J., 2013. Episodic slow slip events in the Japan subduction zone before the 2011 Tohoku-Oki earthquake. Tectonophysics 600, 14–26. http://dx.doi.org/10.1016/j.tecto.2012.08.022.

Kato, A., Obara, K., Igarashi, T., Tsuruoka, H., Nakagawa, S., Hirata, N., 2012. Propagation of slow slip leading up to the 2011 M_w 9.0 Tohoku-Oki earthquake. Science 335, 705–708. http://dx.doi.org/10.1126/science.1215141.

Kato, A., Nakagawa, S., 2014. Multiple slow-slip events during a foreshock sequence of the 2014 Iquique, Chile M_w 8.1 earthquake. Geophys. Res. Lett. 41, 5420–5427. http://dx.doi.org/10.1002/2014GL061138.

Kato, N., Hirasawa, T., 1999. A model for possible crustal deformation prior to a coming large interplate earthquake in the Tokai district, central Japan. Bull. Seismol. Soc. Am. 89, 1401–1417.

Langbein, J., Murray, J.R., Snyder, H.A., 2006. Coseismic and initial postseismic deformation from the 2004 Parkfield, California, earthquake, observed by global positioning system, electronic distance meter, creepmeters, and borehole strainmeters. Bull. Seismol. Soc. Am. 96, S304–S320.

Linde, A., Gladwin, M., Johnston, M., 1996. A slow earthquake sequence on the San Andreas fault. Nature 383, 65–68.

Lohman, R.B., McGuire, J.J., 2007. Earthquake swarms driven by aseismic creep in the Salton Trough, California. J. Geophys. Res. 112, 1–10. http://dx.doi.org/10.1029/2006JB004596.

Matsuzawa, T., Hirose, H., Shibazaki, B., Obara, K., 2010. Modeling short- and long-term slow slip events in the seismic cycles of large subduction earthquakes. J. Geophys. Res., Solid Earth 115, B12301. http://dx.doi.org/10.1029/2010JB007566.

Mazzotti, S., Adams, J., 2004. Variability of near-term probability for the next great earthquake on the Cascadia subduction zone. Bull. Seismol. Soc. Am. 94, 1954–1959.

Montgomery-Brown, E.K., Segall, P., Miklius, A., 2009. Kilauea slow slip events: identification, source inversions, and relation to seismicity. J. Geophys. Res., Solid Earth 114. http://dx.doi.org/10.1029/2008JB006074.

Nadeau, R.M., Guilhem, A., 2009. Nonvolcanic tremor evolution and the San Simeon and Parkfield, California, Earthquakes. Science 325, 191–193. http://dx.doi.org/10.1126/science1174155.

Obara, K., Hirose, H., Yamamizu, F., Kasahara, K., 2004. Episodic slow slip events accompanied by non-volcanic tremors in southwest Japan subduction zone. Geophys. Res. Lett. 31, 4. http://dx.doi.org/10.1029/2004GL020848.

Ozawa, S., Hatanaka, Y., Kaidzu, M., Murakami, M., Imakiire, T., Ishigaki, Y., 2004. Aseismic slip and low-frequency earthquakes in the Bungo channel, southwestern Japan. Geophys. Res. Lett. 31, 1–5. http://dx.doi.org/10.1029/2003GL019381.

Ozawa, S., Suito, H., Tobita, M., 2007. Occurrence of quasi-periodic slow-slip off the east coast of the Boso peninsula, Central Japan. Earth Planets Space 59, 1241. http://dx.doi.org/10.1186/BF03352072.

Perfettini, H., Avouac, J., 2004. Postseismic relaxation driven by brittle creep: a possible mechanism to reconcile geodetic measurements and the decay rate of aftershocks, application to the Chi–Chi. J. Geophys. Res. 109, B02304. http://dx.doi.org/10.1029/2003JB002488.

Roeloffs, E., 2006. Evidence for aseismic deformation rate changes prior to earthquakes. Annu. Rev. Earth Planet. Sci. 34, 591–627. http://dx.doi.org/10.1146/annurev.earth.34.031405.124947.

Rogers, G., Dragert, H., 2003. Episodic tremor and slip on the Cascadia subduction zone: the chatter of silent slip. Science 300, 1942–1943.

Rubinstein, J.L., Vidale, J.E., Gomberg, J., Bodin, P., Creager, K.C., Malone, S.D., 2007. Non-volcanic tremor driven by large transient shear stresses. Nature 448 (7153), 579–582.

Ruiz, S., Metois, M., Fuenzalida, A., Ruiz, J., Leyton, F., Grandin, R., Vigny, C., Madariaga, R., Campos, J., 2014. Intense foreshocks and a slow slip event preceded the 2014 Iquique M_w 8.1 earthquake. Science 345, 165–1169. http://dx.doi.org/10.1126/science1256074.

Scholz, C., Molnar, P., Johnson, T., 1972. Detailed studies of frictional sliding of granite and implications for the earthquake mechanism. J. Geophys. Res. 77, 6392–6406. http://dx.doi.org/10.1029/JB077i032p06392.

Schwartz, S.Y., Rokosky, J.M., 2007. Slow slip events and seismic tremor at circum-Pacific subduction zones. Rev. Geophys. 45. http://dx.doi.org/10.1029/2006RG000208.

Segall, P., Bradley, A.M., 2012. Slow-slip evolves into megathrust earthquakes in 2D numerical simulations. Geophys. Res. Lett. 39, L18308. http://dx.doi.org/10.1029/2012GL052811.

Shelly, D.R., 2009. Possible deep fault slip preceding the 2004 Parkfield earthquake, inferred from detailed observations of tectonic tremor. Geophys. Res. Lett. 36, L17318. http://dx.doi.org/10.1029/2009GL039589.

Shelly, D.R., Beroza, G.C., Ide, S., 2007. Non-volcanic tremor and low-frequency earthquake swarms. Nature 446, 305–307. http://dx.doi.org/10.1038/nature05666.

Sit, S., Brudzinski, M., Kao, H., 2012. Detecting tectonic tremor through frequency scanning at a single station: application to the Cascadia margin. Earth Planet. Sci. Lett. 353–354, 134–144. http://dx.doi.org/10.1016/j.epsl.2012.08.002.

Skoumal, R.J., Brudzinski, M.R., Currie, B.S., 2015. Distinguishing induced seismicity from natural seismicity in Ohio: demonstrating the utility of waveform template matching. J. Geophys. Res. 120. http://dx.doi.org/10.1002/2015JB012265.

Skoumal, R.J., Brudzinski, M.R., Currie, B.S., 2016. An efficient repeating signal detector to investigate earthquake swarms. J. Geophys. Res. http://dx.doi.org/10.1002/2016JB012981.

Thomas, A.M., Nadeau, R.M., Bürgmann, R., 2009. Tremor-tide correlations and near-lithostatic pore pressure on the deep San Andreas fault. Nature 462, 1048–1051. http://dx.doi.org/10.1038/nature08654.

Tse, S.T., Rice, J.R., 1986. Crustal earthquake instability in relation to the depth variation of frictional slip properties. J. Geophys. Res. 91, 9452–9472.

Uchida, N., Hasegawa, A., Matsuzawa, T., Igarashi, T., 2004. Pre- and post-seismic slow slip on the plate boundary off Sanriku, NE Japan associated with three interplate earthquakes as estimated from small repeating earthquake data. Tectonophysics 385, 1–15.

Universidad Nacional Autonoma de Mexico (UNAM) Seismology Group, 2013. Ometepec-Pinotepa Nacional, Mexico earthquake of 20 March 2012 (Mw 7.5): a preliminary report. Geofís. Int. 52 (2), 173–196.

Vallée, M., Nocquet, J.-M., Battaglia, J., Font, Y., Segovia, M., Régnier, M., Mothes, P., Jarrin, P., Cisneros, D., Vaca, S., Yepes, H., Martin, X., Béthoux, N., Chlieh, M., 2013. Intense interface seismicity triggered by a shallow slow slip event in the Central Ecuador subduction zone. J. Geophys. Res., Solid Earth 118. http://dx.doi.org/10.1002/jgrb.50216.

Vidale, J.E., Hotovec, A.J., Ghosh, A., Creager, K.C., Gomberg, J., 2011. Tiny intraplate earthquakes triggered by nearby episodic tremor and slip in Cascadia. Geochem. Geophys. Geosyst. 12. http://dx.doi.org/10.1029/2011GC003559.

Walter, J.I., Meng, X., Peng, Z., Schwartz, S.Y., Newman, A.V., Protti, M., 2015. Far-field triggering of foreshocks near the nucleation zone of the 5 September 2012 (M_w 7.6) Nicoya Peninsula, Costa Rica earthquake. Earth Planet. Sci. Lett. 431, 75–86. http://dx.doi.org/10.1016/j.epsl.2015.09.017.